Published online 26 May 2016

Nucleic Acids Research, 2016, Vol. 44, No. 14 ***e125***
doi: 10.1093/nar/gkw478

Examining cooperative binding of Sox2 on DC5 regulatory element upon complex formation with Pax6 through excess electron transfer assay

Abhijit Saha[1], Seiichiro Kizaki[1], Debojyoti De[2], Masayuki Endo[3], Kyeong Kyu Kim[2,*] and Hiroshi Sugiyama[1,3,*]

[1]Department of Chemistry, Graduate School of Science, Kyoto University, Kitashirakawa-Oiwakecho, Sakyo-Ku, Kyoto 606-8502, Japan, [2]Department of Molecular Cell Biology, Sungkyunkwan University, School of Medicine, Suwon 440-746, Korea and [3]Institute for Integrated Cell-Materials Sciences (iCeMS) Kyoto University, Yoshida-ushinomiyacho, Sakyo-Ku, Kyoto 606-8501, Japan

Received November 16, 2015; Revised May 12, 2016; Accepted May 17, 2016

ABSTRACT

Functional cooperativity among transcription factors on regulatory genetic elements is pivotal for milestone decision-making in various cellular processes including mammalian development. However, their molecular interaction during the cooperative binding cannot be precisely understood due to lack of efficient tools for the analyses of protein–DNA interaction in the transcription complex. Here, we demonstrate that photoinduced excess electron transfer assay can be used for analysing cooperativity of proteins in transcription complex using cooperative binding of Pax6 to Sox2 on the regulatory DNA element (DC5 enhancer) as an example. In this assay, ^{Br}U-labelled DC5 was introduced for the efficient detection of transferred electrons from Sox2 and Pax6 to the DNA, and guanine base in the complementary strand was replaced with hypoxanthine (I) to block intra-strand electron transfer at the Sox2-binding site. By examining DNA cleavage occurred as a result of the electron transfer process, from tryptophan residues of Sox2 and Pax6 to DNA after irradiation at 280 nm, we not only confirmed their binding to DNA but also observed their increased occupancy on DC5 with respect to that of Sox2 and Pax6 alone as a result of their cooperative interaction.

INTRODUCTION

The complexity of an organ development is manifested through spatiotemporal expression of genes involved in development, which is tightly regulated to a large extent by the combination of transcription factors in multi-protein complexes (1–13). In these processes, the binding affinity of transcription factors to their genetic elements, which is crucial for transcription activity, is modulated by cooperative binding: low inherent binding affinity of the individual factors is largely enhanced when they present together by their synergistic action. One example that shows this plasticity and diverse combinatorial transcription activity is Sox2, which activates its downstream transcriptional targets by forming cooperative complex with various factors in each developmental stage. For example, it maintains pluripotency by partnering with various factors like Oct4 and Nanog (5,7,11–12), and controls neurogenesis and retinal developmental by forming complexes with Pax6 (7–10), Otx2 (11), Tlx (12) or Brn2 (13). Therefore, it is essential to investigate the dynamics of their cooperativity to understand functional intricacies involved in the process of transcription.

Electrophoretic mobility shift assay (EMSA) widely used for probing the cooperativity and synergistic activity of transcription factors, is often very time consuming and comes with varying sensitivity. Most importantly, observing the ternary complex between co-existing proteins and DNA is not straightforward because, in many cases, the partner transcription factors interact with low affinity, which limits the possibility to run the intact complex through the gel even at low temperature. In addition, this method cannot provide any detailed molecular mechanism of cooperative binding. Alternatively, high-resolution structural studies such as protein crystallography and nuclear magnetic resonance can surely give the picture for understanding cooperativity of transcriptional complex, but these methods have limitation in term of sample preparation and technical difficulty. Therefore, there is a need of quick, sensitive, and reproducible alternative method to determine cooperativity of transcription factors in detail. Here, we propose that photoinduced excess electron transfer (EET) from the trypto-

*To whom correspondence should be addressed. Tel: +81 75 753 4002; Fax: +81 75 753 3670; Email: hs@kuchem.kyoto-u.ac.jp
Correspondence may also be addressed to Kyeong Kyu Kim. Tel: +82 31 299 6136; Fax: +82 31 299 6269; Email: kyeongkyu@skku.edu

phan residues of protein to ^{Br}U labelled DNA is an alternative to the classical ways to probe cooperativity by examining the synergistic action of Sox2 and Pax6 on their putative regulatory genetic element called DC5. Transcription factor Pax6 initiates lens development by forming a cooperative complex with Sox2 on the DC5 element, which enhances the lens specific expression of the δ-crystallin gene (Figure 1A). This specific alliance is responsible for the development of neuronal and retinal tissues (7–10). For instance, when the Pax6 binding sequence of the DC5 enhancer is replaced with Pax6 binding consensus (DC5con, Figure 1A) the cooperation in binding between Sox2 and Pax6 decreases and the complex failed to activate the reporter gene. Previously, formation of this functional ternary complex was shown by classical EMSA (7,8) and it was recently analysed by atomic force microscopy (AFM) on a DNA origami frame (14). Although DNA origami is an attractive platform to observe these complex biological events, the facilities and technical knowledge required to prepare DNA origami frames are available to only a limited number of laboratories. Thus, our proposed method can be used in many cases to detect such crucial biological events based on photosensitive platform.

Long-range EET leads to a great deal of redox chemistry that is widely observed in key biological events such as signalling and sensing (15). This long-range electron transfer is possible within a distance of 10–25 Å in biological redox reactions (16). It has been proposed that some repair enzymes use electron transfer from redox cofactors to allow the detection of DNA lesions generated by the oxidation at remote site (17–19). However, it was also observed that EET can go through without redox cofactors as evidenced in the case of *Escherichia coli* DNA photolyase that can repair thymine dimers without the aid of redox cofactors (20,21). Moreover, it was also reported that thymine dimers can be repaired by Lys-Trp-Lys motif under irradiation conditions (22–25). These results together suggest that specific amino acids are responsible for the repair process through EET. Requirement of specific amino acids as electron donor was further supported in a previous report where it was observed that the photoreactivity of DNA can be achieved by the photoinduced single-electron transfer from Trp residue of the DNA binding protein using an electron acceptor, ^{Br}U base (25,26). Based on these results, we hypothesized that photoinduced electron transfer from proteins to DNA could be applied to check the specific interaction between protein and DNA, and can be further utilized to probe cooperativity of proteins in transcription complex. To test this possibility, we applied our strategy to detect protein–DNA interaction conducted by Sox2 or Pax6 alone or in their complex. We modified DC5 element and DC5 Con by replacing thymine with its ^{Br}U analogue at the binding site of the protein. ^{Br}U is an attractive synthetic nucleotide as its substitution does not affect the functionality of the resulting DNA but can easily trap an electron during DNA-mediated EET. The trapped excess electron converts ^{Br}U to a uracil-5-yl radical (U$^{\bullet}$) by eliminating the bromide ion (27). As a result, EET from protein to ^{Br}U results in the strand cleavage by the heat treatment since the heat-labile 2-deoxyribonolactone is generated from U$^{\bullet}$ radical by intrastrand hydrogen abstraction from the deoxyribose moiety of the 5′-side at the C1′ and C2α′ position, respectively (28,29). The strand cleavage can be accelerated further by including isopropanol (^{i}PrOH) as an excess H-atom source and subsequent treatment of uracil-DNA-glycosylase (UDG) as previous reported (30,31). Under this strategy, Sox2- or Pax6 and their cooperative binding to DNA can be monitored by the strand cleavage due to trapping of excess electrons from tryptophan residues to ^{Br}U. For this purpose, we used purified recombinant DNA-binding domains: Sox2(HMG), HMG representing high-mobility group, and Pax6(DBD), DBD representing DNA-binding domain.

MATERIALS AND METHODS

General

Preparation of DNA. All the oligos were purchased from Jbios and Sigma Genosys and used without further purification.

Preparation of Sox2 and Pax6. These two proteins were amplified in a similar way as before (14). The gene encoding the HMG domain (residues, 1–117) of human Sox2 was amplified and cloned in pVFT1S using EcoR1 and Xho1 sites. And, the gene encoding the DNA binding domain (residues 4–169) of human Pax6 was amplified and cloned into pET41a (Novagen, Darmstadt, Germany) using Nco1 and Xho1 sites. *E. coli* BL21 (DE3) Star (Invitrogen, CA, USA) transformed with pVFT1S-Sox2(HMG) and pET41a-Pax6(DBD) were grown in LB media containing Kanamycin (Duchefa Biochemie, The Netherlands) at a concentration of 50 μg/ml. Both cultures were grown for 12 h and then diluted 1:100 into fresh LB media and incubated at 37°C with shaking until the OD 600 was 1.0. Cells were then induced with a final concentration of 0.5 mM isopropyl-β-D-thiogalactopyranoside (IPTG) (EMD Chemicals, CA, USA) and incubated for 6 h. Cells were harvested by centrifugation at 5000 rpm for 15 min at 4°C and stored at −80°C until used. Cell pellets expressing Sox2(HMG) were suspended in buffer A (25 mM Tris–Cl, pH 8.0, 500 mM NaCl, 40 mM imidazole and 1 mM PMSF) and disrupted with a vibracell sonicator (Sonics & Materials Inc., CN, USA) using a pulse of 2 s ON and 4 s OFF for a total of 10 min at an amplitude of 60%. Cell lysate was clarified by centrifugation at 30 000 *g* for 90 min at 4°C. The supernatant was applied to a nickelcharged NTA column (GE Healthcare, NJ, USA) pre-equilibrated with buffer B (25 mM Tris–HCl, pH 8.0, 500 mM NaCl, 40 mM imidazole). The column was washed with ten column volumes (CV) of buffer B, and the protein was eluted with a gradient from 40 mM to 1 M imidazole in 40 CV. The fractions containing Sox2(HMG) were concentrated to <5 ml using a centrifuge filtration device Vivaspin 20 (Sartorius Stedim Biotech, Goettingen, Germany) and then applied to a Superdex 200 column (GE Healthcare, NJ, USA) equilibrated with buffer C (25 mM Tris–HCl, pH 8.0, 500 mM NaCl, 1 mM DTT). Cell pellets expressing GST-Pax6(DBD) were suspended in buffer D (25 mM Tris–HCl, pH 7.5, 500 mM NaCl, 40 mM imidazole and 1 mM PMSF) and disrupted with a vibracell sonicator (Sonics & Materials Inc., CN, USA) using a pulse of 2 s ON and 4 s OFF for a total of

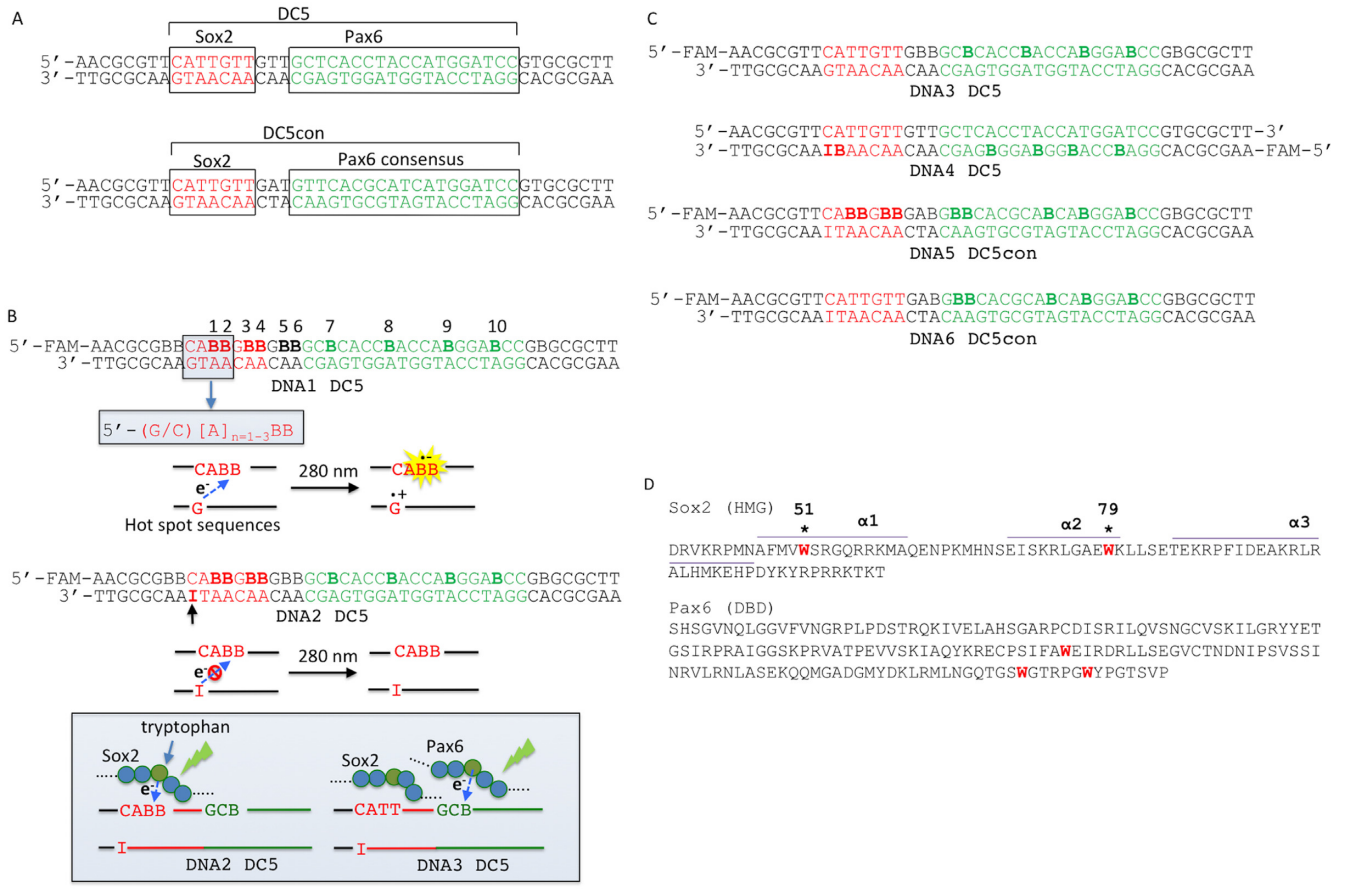

Figure 1. (**A**) DC5 enhancer element of δ-crystallin gene, in which Sox2 and Pax6 interact during the transcription process leading to the development of neuronal and retinal tissues. The binding sites of Sox2 and Pax6 are shown in red and green, respectively. Also shown the sequence when the DC5 enhancer is replaced with Pax6 binding consensus (DC5con). (**B**) DC5 element was modified into DNA1 by replacing thymine residues with its analogous ^{Br}U residues (B represents ^{Br}U) in one strand to capture the excess electrons from the protein. But the motif 5′-CABB in the Sox2-binding site of DNA1 is known for 'Hot-spot' which is labile for intra-strand electron transfer as shown in the figure. Therefore, DNA1 was further modified to DNA2 by replacing G with hypoxanthine (I) (indicated by an arrow in DNA2) to prevent intrastrand electron transfer. Also shown the schematic representation of the photoinduced electron transfer from the excited state of tryptophan residues of Sox2 alone (left) and Sox2 with its partner Pax6 to the DC5 DNA element (right). (**C**) DNA3 was designed to capture an electron from Pax6 by replacing 'T' with '^{Br}U' in the Pax6 binding sites as shown in (B, right). DNA4 was designed to check the photoreactivity of the complementary strand by incorporating ^{Br}U residues. DNA5 and DNA6 were designed based on DC5con sequence (**D**) The amino acid sequences of Sox2(HMG) and Pax6(DBD) are shown. Trp residues are shown red.

10 min at an amplitude of 60%. The cell lysate was clarified by centrifugation at 30 000 *g* for 90 min at 4°C. The supernatant was applied to a nickel-charged NTA column (GE Healthcare, NJ, USA) pre-equilibrated with buffer D. The column was washed with 10 CV of buffer B, and the protein was eluted with a gradient from 40 mM to 1 M imidazole in 50 CV. The fractions containing Pax6(DBD) were concentrated using a centrifuge filtration device Vivaspin 20 (Sartorius Stedim Biotech, Goettingen, Germany). The proteins were then moved to buffer E (25 mM Tris–HCl, pH 7.5, 500 mM NaCl, 1 mM DTT).

Irradiation set up. HM-3 hypermonochromator (Jasco) was used for irradiation at 280 nm. The eppendorf tube containing the sample (DNA and protein) was attached vertically with the light fiber using a holder so that the light can pass through the sample and placed in an ice box. The description of the machine used in this study can be found at reference (32).

Photoreaction scheme. DNA and protein were mixed in a buffer containing 10 mM Tris–HCl pH 7.5, 1 mM ethylenediaminetetraacetic acid (EDTA), 50 mM KCl, 100 μg/ml bovine serum albumin, 5% v/v glycerol and 200 mM ^{i}PrOH. The sample was incubated at 4°C for minimum 1 h and then irradiated using 280 nm UV transilluminator. The sample was treated with UDG enzyme (1.25 U), incubated at 37°C for 1 h. After the enzymatic digestion the sample was dried up completely using high vacuum pump and to it about 10 μL of loading dye (containing of 300 μl of 0.5 M EDTA, 200 μl of Milli-Q water, 10 ml of formamide and 2.5 mg of new fuchsin) were added and finally heated at 95°C for 10 min. The sample was then analysed by denaturing polyacrylamide gel electrophoresis (PAGE) (20%).

Fluorescence measurements. Steady-state fluorescence measurements of photoirradiated Sox2 and Pax6 samples were conducted with a Jasco FP-6300 spectrofluorometer. Measurements were performed by using a fluorescence cell

with a 0.5-cm path length. Fluorescent intensity of Sox2 was quenched when it forms a complex with DNA2, it was difficult to estimate the conversion of the Trp in Sox2. To overcome this trouble, we added a high concentration of NaCl (2 M final concentration) to the reaction mixture after the photo irradiation and checked the fluorescent intensity after keeping the solution in ice for at least 30 min. Gradually, the fluorescence intensity of the Trp is recovered (∼90–95%) because Sox2 cannot bind to DNA in such high-salt conditions. The fluorescence intensity of the Trp of Sox2 was not affected in these conditions. A similar condition was used for Pax6.

PAGE. After photoreaction cleaved DNA was analysed in a 20% polyacrylamide denaturing gel (7 M Urea). The condition of electrophoresis was 200 V and 250 mA for 140 min. For **EMSA,** the electrophoresis condition was 80 V and 140 mA for 80 min. The gel was analysed by FLA-3000 (Fujifilm) and the cleavage amount was measured by using multigauge v3.1 software.

Model building

The model of hSox2(HMG) bound to DC5 element was made using coordinates of hSox2(HMG) in the structure of hSox2/FGF4 (PDB ID: 1GT0) and the DNA corresponding to DC5 Sox2 DNA element in the structure of SRY(HMG)/DC5 (PDB ID: 2GZK) by superposing the hSox2(HMG) on SRY in 2GZK followed by manual modelling and energy minimization to get a pose of possible interaction of hSox2(HMG) with DC5 Sox2 DNA element.

RESULTS

Designing DC5 by incorporating ^{Br}U and hypoxanthine (I) to capture an electron from Sox2(HMG) or Pax6(DBD)

We first designed DNA1, a double strand DC5 element containing ^{Br}U residues at the binding site of Sox2 and Pax6 (Figure 1B). We expected that DNA1 would capture electrons at the respective protein binding sites due to close proximity of any of the tryptophan residues of the binding protein when incubated with proteins under UV irradiation (Figure 1D). But it is known that specific sequences in the ^{Br}U substituted DNA, for instance, 5′-G/C[A]$_{n=1,2,3}$^{Br}U^{Br}U-3′ sequences, called hot-spots can induce intra-strand electron transfer under UV irradiation condition (33,34). Since G has the lowest oxidation potential among the four bases (The oxidation potentials of G, A, T, C are 1.24, 1.69, 1.9, 1.9 V, respectively (35)), an electron from G transfers to ^{Br}U^{Br}U residues through intervening A bridges adjacent to ^{Br}U (as shown in the Figure 1B) and A bridges in this case helps in forward and backward electron transfer process (33,34). A same hot-spot sequence, CA^{Br}U^{Br}U was found in the Sox2 binding sequence while in the Pax6 binding site (in both cases DC5 and DC5con) no such sequences was noticed (even though there are many G's but lacks A bridges between G and ^{Br}U^{Br}U). To quench this intra-strand electron transfer from G to ^{Br}U ^{Br}U in the Sox2 binding site of DNA1 and to eliminate unintended false positives, we constructed DNA2 (Figure 1B) in which G was replaced by hypoxanthine (I), a modified purine base, in its complementary strand (indicated by an arrow) only in the Sox2 site. We hypothesized that this modification would prevent any intra-strand electron transfer due to the higher oxidation potential of I than that of G (1.4 versus 1.24 V) as depicted in a schematic representation shown in Figure 1B (down) (35). To test this principle, we irradiated DNA1 and DNA2 at 280 nm for 30 min and analysed the resulting samples by denaturing gel electrophoresis (Supplementary Figure S1). While DNA1 got cleaved, almost no cleavage was observed in DNA2, suggesting the absence of intra-strand electron transfer. Therefore, this method was employed in other assays to eliminate any false readout in the hot spot. This exercise was not necessary for Pax6 binding site due to lack of similar hot spots (Figure 1A). To examine whether DNA2 limits DNA binding capacity of Sox2, we performed EMSA using Sox2(HMG) on DNA2 and compared with unmodified DC5. We observed Sox2(HMG) binds to DNA2 in almost similar stoichiometric ratio to unmodified DC5 (Supplementary Figure S2).

Capturing an electron from Sox2(HMG) upon binding to DNA

We checked the photoreactivity of DNA2 upon treatment of Sox2(HMG) at a molar ratio of 2:1 and 5:1 (protein:DNA) under irradiation at 280 nm for 15 min at 0°C in a buffer containing Tris–HCl pH 7.5 and 200 mM ^{i}PrOH. After irradiation, the sample was subjected to UDG treatment for converting U into the heat-labile abasic site (AP site). When the sample was heat treated at 95°C for cleavage and analysed by 20% denaturing PAGE, two distinct DNA fragments was observed (lane 5 in Figure 2). Based on the size of the fragments, they were expected to be the cleavage products at the Sox2-binding site (indicated by arrows in Figure 2). This interpretation is further confirmed by the increased band intensity when DNA2 was incubated with the higher concentration of Sox2(HMG) (lane 6 in Figure 2). Interestingly, no DNA cleave was detected other than at the Sox2-binding site, manifesting that Sox2 binding to the DC5 element is sequence specific. It should be noted that there was no strand cleavage in absence of Sox2(HMG) under the same reaction condition (lane 4 in Figure 2). Taken together, it can be concluded that the photoinduced electron transfer from protein to DNA and subsequent cleavage of DNA can be used for investigating sequence specific binding of transcription factors to their corresponding DNA elements.

Locating the tryptophan residues of Sox2(HMG)

To get a clear view of placement of electron donor–acceptor couples within the protein–DNA complex, a model of human Sox2(HMG) bound to 5′-CA^{Br}U^{Br}UG^{Br}U^{Br}U-3′/5′-GTAACAA-3′ was constructed by placing the hSox2(HMG) to the DC5 element (5′-CATTGTT-3′/5′-GTAACAA-3′) after replacing thymine with ^{Br}U (see 'Materials and Methods' section). The complex model reveals that the first two helices comprising 45 residues in the HMG domain are involved in the sequence-specific binding to the minor-groove of DNA (Figure 3). Inspection of the crystal structure inferred that both W51 and W79

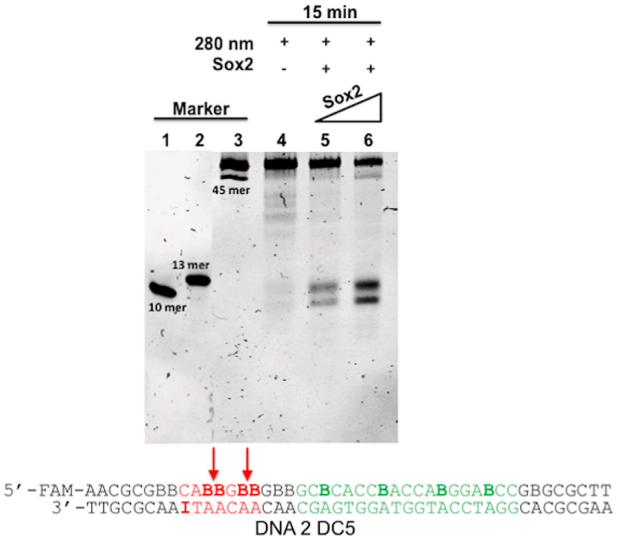

Figure 2. Analyses of the DNA cleavage as a result of photoinduced electron transfer from Sox2(HMG) to the modified DC5 element (DNA2) using 20% polyacrylamide denaturing gel (7 M urea). The gel electrophoresis was performed at 200 V and 250 mA for 140 min and checked by Fujifilm (FLA-3000). Lanes 1, 2 and 3 are DNA size markers with sizes of 45, 10 and 13 mer respectively. Lane 4, DNA2 with UV irradiation at 280 nm for 15 min; lane 5, UV irradiation at 280 nm for 15 min on Sox2(HMG): DNA2 at 2.5:1.25 μM ratio, lane 6, UV irradiation at 280 nm for 15 min on Sox2(HMG): DNA2 at 6.25:1.25 μM ratio. Concentration of DNA was 1.25 μM. Reaction was performed in a buffer containing 10 mM Tris–HCl pH 7.5, 1 mM EDTA, 50 mM KCl, 100 μg/ml bovine serum albumin, 5% v/v glycerol and 200 mM ^{i}PrOH. Each sample was incubated with 1.25 U of UDG at 37°C for 1 h after irradiation and finally heated at 95°C for 10 min.

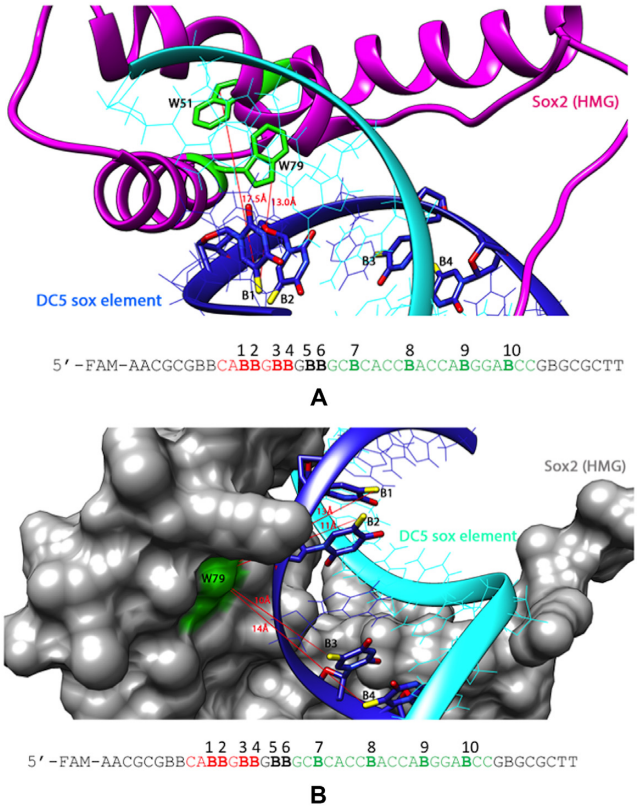

Figure 3. (**A**) Ribbon diagram of hSox2(HMG) bound to 5′-CAB1B2GB3B4-3′/5′-AACAATG-3′ which was constructed based on the structure of human Sox2(HMG) and structure of DC5 Sox2 DNA element shown below. B base represents ^{Br}U. Tryptophan residues (W51 and W79) and ^{Br}U nucleosides (B1–B4) are drawn as green and blue stick models, respectively, and Br and oxygen atoms in ^{Br}U are shown in yellow and red, respectively. (**B**) Surface representation of hSox2(HMG) bound to 5′-CAB1B2GB3B4-3′/5′-AACAATG-3′. B represents ^{Br}U. Tryptophan residue (W79) and ^{Br}U nucleotides (B1-B4) are coloured in green and blue, respectively, and Br and oxygen atoms in ^{Br}U are shown in yellow and red, respectively. The sequence is shown below.

located near the DNA–protein interface are in close proximity to each other (Figure 3A). As a result, tryptophan residues, W51 and W79, are located close to the electron acceptor ^{Br}U (B1 and B2) at distances of 17.5 and 13.0 Å, respectively, which are within the range of distance for potent electron transfer. We anticipate that both the tryptophan residues are putative electron donors but W79 might play a major role in the photoreactivity considering their orientation and distance. From the surface representation of Sox2(HMG) in the model, it can be inferred that W79 located on the DNA-protein interface is in close proximity to the electron acceptor ^{Br}U (B1 and B2) at distances of 13 and 11 Å, respectively (Figure 3B). In addition, W79 seems to also transfer the electrons to B3 and B4 as well, since distances from indole nitrogen of W79 to bromine are 10 and 14 Å, respectively (Figure 3B). However, W51 appears to be located on the surface opposite to that of protein–DNA interface and thus it might have less electron transfer propensity.

Capturing an electron from Pax6(DBD) upon complex formation with Sox2(HMG) and DNA3

We then designed DNA3 to capture the transferred electrons from Pax6 by substituting thymine with ^{Br}U in the Pax6 binding region (Figure 1C). The photoreactivity of DNA3 was examined similarly in the presence of either Pax6(DBD) alone or in combination of Pax6(DBD) with Sox2(HMG) (Figure 4). It is well known that that most of the transcription co-activators of Sox2 have low inherent DNA binding affinity in the absence of Sox2 but gain affinity when they form a ternary complex in the presence of Sox2. As expected, Pax6(DBD) alone was not able to induce any DNA cleavage, representing that electrons were not transferred from the tryptophan residues of Pax6 to DNA possibly due to the transient binding of protein to DNA (lane 5 in Figure 4). However, in the presence of both Sox2(HMG) and Pax6(DBD), electron transfer from Pax6 led to strand cleavage (lane 6 in Figure 4). Pax6(DBD) contains three Trp residues, and thus it cannot be concluded that which residues are involved in electron transfer due to the lack of high resolution model of Pax6/DC5 complex. However, it is obvious that one of Trp residues of Pax6 approaches to proximal position to ^{Br}U by forming a stable complex with DNA due to the conformation change accompanied by Sox2 binding. The cooperative binding of Sox2–Pax6 on DNA3 and increased DNA binding affinity of Pax6

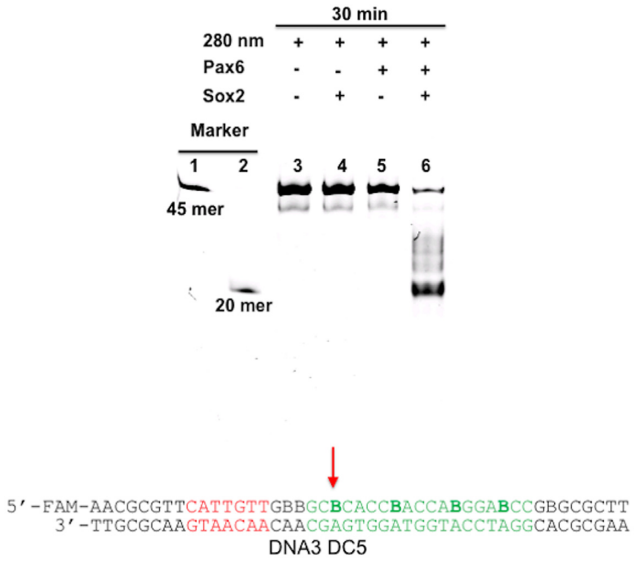

Figure 4. Analyses of DNA cleavage by photoinduced electron transfer from Pax6(DBD) to DNA3 in the Sox2–Pax6–DNA3 complex using 20% polyacrylamide denaturing gel (7 M urea). Lane 1, 45 mer DNA marker; lane 2, 20 mer DNA marker; lane 3, UV irradiated DNA3 at 280 nm for 30 min; lane 4, UV irradiated DNA3 with 6.25 μM of Sox2, lane 5, UV irradiated DNA3 with 6.25 μM of Pax6; lane 6, UV irradiated DNA3 with 6.25 μM of Sox2 and Pax6; The concentration of DNA3 was 1.25 μM in all samples. The reaction conditions are same as Figure 3.

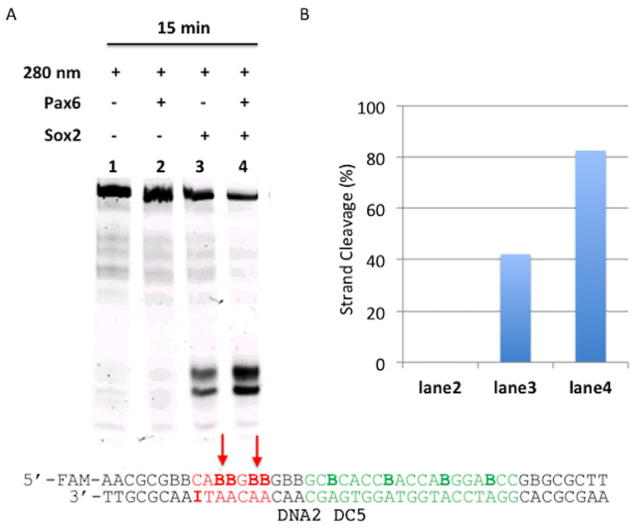

Figure 5. (**A**) The analyses of the DNA cleavage by photoelectron transfer from Sox2 to DNA in the presence of Pax6. The photoreaction procedure is described in Figure 3. Lane 1, DNA2 irradiated by UV 280 nm for 15 min; lane 2, Pax6(DBD) (2.5 μM) in lane 1 condition; lane 3, Sox2(HMG) (2.5 μM) in the lane 1 condition; Lane 3, Sox2(HMG) (2.5 μM) and Pax6(DBD) (0.625 μM) in the lane 1 condition. The concentration of DNA2 was 1.25 μM in all samples. (**B**) Quantification of the extent of strand cleavage shown in lanes 2, 3 and 4.

were also confirmed by a conventional EMSA (Supplementary Figure S3), which validated the result of EET assay.

Validating the influence of Pax6(DBD) on Sox2(HMG) binding by electron transfer

It has been demonstrated that Pax6 enhances the binding affinity of Sox2 to DC5 by AFM on a DNA origami frame (14). To confirm the enhanced binding affinity of Sox2 upon cooperative binding of Pax6 using EET assay, we investigated the electron transfer from Sox2 to DNA2 in the presence and absence of Pax6 under irradiation conditions by examining the DNA cleavage (Figure 5). DNA2 was incubated with Sox2(HMG) alone or with Sox2(HMG)/Pax6(DBD) and irradiated for 15 min following the similar photoreaction procedure in Figure 2, and the amount of the cleavage DNA was compared. To assess the extent of any synergistic effect, we added a minimum amount of Pax6 (0.5 equiv.) to a sample containing two equivalent Sox2, thus to ensure that at this amount it should not cleave the DNA at its binding site. Consistently with the previous report confirmed by AFM, the DNA binding affinity of Sox2 was enhanced about two folds by Pax6 binding as manifested by the increased cleavage content from 42.1 to 82.5% before and after Pax6 binding, respectively. It is to be noted that Pax6 alone (lane 2) at 2 equiv. was unable to give any cleavage. This result suggests that, like Sox2, Pax6 also plays an important role in stabilizing the protein/DNA complex. Given that strand cleavage through electron transfer from Sox2–Pax6 to DNA is more extensive than that from Sox2 or Pax6 alone, it is clear that a cooperative binding partnership is in operation.

Electron transfer from Pax6(DBD) on DC5con: determining the structure–function relationship between DC5 and DC5con

Because it has been found that DNA molecule commonly plays an active role in cooperative interactions thus we were interested to see whether EET can help in finding the structure–function relationship or not (36). One such example is the replacement of Pax6 binding sequence from the DC5 enhancer with Pax6 binding consensus as shown in Figure 1A, results in the disruption of cooperation between Pax6 and Sox2. As a result the complex could not activate the reporter gene (7). In order to probe this crucial structure–function relationship using EET we modified the DC5con by DNA5 and DNA6 (Figure 1A and C). We designed DNA5 by replacing thymine with ^{Br}U in the DC5con sequence to confirm EET by Sox2. Our results revealed that Sox2 alone was able to cleave DNA5 as shown in Figure 6 (lane 6). Since there is a possibility that Sox2 may degrade by the electron injection (oxidation of tryptophan) to DNA5 thus it may disturb the formation of ternary complex. That is why we decided to design DNA6 in which thymine was replaced with ^{Br}U only in the Pax6 binding site. A similar strategy was applied with DNA2 (DC5 sequence) which was used for Sox2 (Figure 2) while a different DNA3 was used for Pax6 induced EET (Figure 4). Interestingly in the DC5con, we revealed that Pax6 alone cleaved the DNA6 at 17.5% at its binding site (Figure 6, lane 8) while in case of DC5 no such cleavage was seen (Figure 4, lane 5). When we added Sox2 and Pax6 with DNA6 we observe that it induces strand cleavage higher than Pax6 alone (lane 9) which indicates that still the cooperativity is active but less compare to DC5.

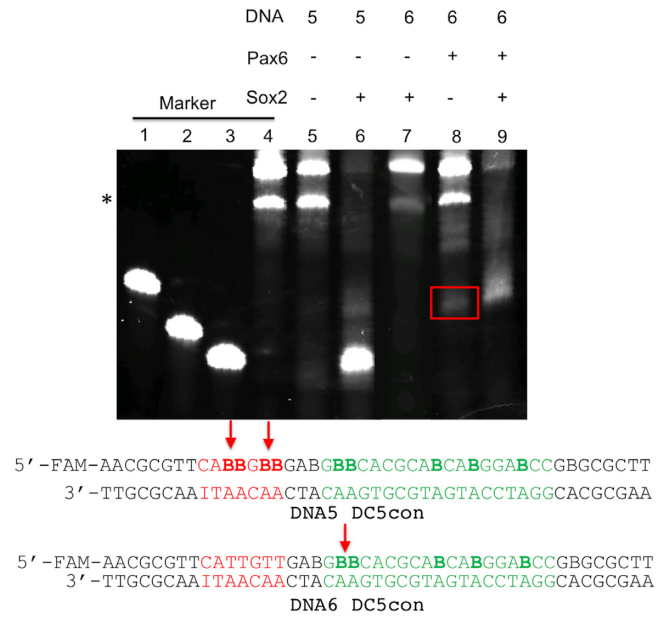

Figure 6. Analyses of DNA cleavage by photoinduced electron transfer from Sox2(HMG) and Pax6(DBD) to DC5Con sequence (DNA5-6) using 15% TBE-Urea Gel (Invitrogen), 180 V, 90 min. Lane 1, 20 mer DNA marker; lane 2, 14 mer DNA marker; lane 3, 11 mer DNA marker; lane 4, 45 mer marker, lane 5, UV irradiated DNA5 at 280 nm for 30 min; lane 6, UV irradiated DNA5 with 6.25 μM of Sox2, lane 7, UV irradiated DNA6 with 6.25 μM of Pax6; lane 8, UV irradiated DNA6 with 6.25 μM of Sox2 and Pax6. The concentration of DNA was 1.25 μM in all samples. Asterisk represents an impurity and it is not generated by photoreaction (because it is seen in control lane 4).

Examining the fate of tryptophan residues after electron injection

Finally, we examined the fate of the tryptophan residues of Sox2 after electron injection into the DNA. Previously, we reported that the fluorescence intensity of tryptophan in Sso7d was quenched after electron transfer to DNA (26). We were thus interested to know the fate of the tryptophan residues of both proteins after irradiation at 280 nm. Upon excitation at 295 nm both Sox2(HMG) and Pax6(DBD) release a characteristic emission peak from tryptophan at 330 and 350 nm, respectively. Interestingly, a significant loss of fluorescence intensity of tryptophan residues of Sox2(HMG) was observed after irradiation for 15 min, as shown in Figure 7A. The loss of emission at 330 nm indicates the photo-degradation in tryptophan residues. In contrast, no significant loss of fluorescence intensity except a little quenching caused by the direct binding was observed in the tryptophan residues of Sox2(HMG) after irradiating the DC5 DNA element that has no ^{Br}U residues. The fluorescent intensity of tryptophan was recovered after adding high concentration of NaCl (2.0 M) into the reaction mixture. This result suggests that electron transfer occurs from Sox2(HMG) to the ^{Br}U residues of DNA2. In contrast, the intensity of fluorescence of Pax6 with DNA2 was not affected even after 30 min irradiation, confirming that no electron transfer from the protein occurs due to the weak binding affinity of Pax6 to DNA2.

DISCUSSION

Multi-protein alliances of specific transcription factors play an important role in mammalian development. However, their characterization suffers from serious hurdles due to the absence of simple and accurate tools to analyse the interaction among the partner transcription factors in maximum cases. Here, we introduced an EET assay that is applied for the first time to characterize the cooperativity between Sox2 and Pax6, key transcription factors involved in development, on the regulatory element DC5. We proposed that EET from protein to DNA could be an alternative way to study such cooperativity. Because of proteins containing tryptophan residues can act as an efficient electron donor under irradiation condition. On the other hand, previously we studied UV irradiated ^{Br}U substituted DNA, and our results revealed photoinduced intra-strand electron transfer process from G to ^{Br}U residue through intervening A bridges in the hot-spot sequences (31,33–34). However, this intra-strand electron transfer is blocked by the incorporation of hypoxanthine residue (I) instead of G. This breakthrough finding opens up the application of ^{Br}U labelled DNA to capture an electron from protein like Sox2(HMG) which binds to a hot-spot containing sequence (Figure 1 and Supplementary Figure S1). From the result it was evident that our designed DNA2 could successfully trap an electron from the tryptophan residues of Sox2(HMG) (Figures 1–3). Again to show electron transfer from Pax6(DBD) we designed DNA3 which contain ^{Br}U only at the Pax6(DBD) binding site. From our result it is further confirmed a photoinduced electron transfer from tryptophan residues of Pax6(DBD) to DNA3 only in the presence of its partner Sox2(HMG) (Figure 5). By electron transfer we also confirmed their increased occupancy on DC5 regulatory element as a result of their cooperative binding than Sox2(HMG) or Pax6(DBD) alone. This new tool of detecting crucial biological events is highly sensitive. The current approach also can provide critical information of protein–nucleic acid interactions. Since it is evident that DNA4 exhibited no photo-reactivity, which contain ^{Br}U only on its complementary strand thus it infer a weak interaction in that strand. Further we extended our study by performing photoreaction on DC5con sequence. The results revealed a low cooperativity in DC5con. Thus, altogether these results suggest that EET can be a useful tool for studying such dynamic protein–nucleic acid interactions.

CONCLUSIONS

To summarize, we demonstrate the characteristic features of cooperativity of Sox2 and its partner Pax6 during the formation of a functional ternary complex with DC5 DNA element by examining electron transfer processes. This approach involved selected substitution of thymine with ^{Br}U residues at the protein-binding sites on the DC5 element and confirmation of binding by the cleavage of the ^{Br}U-substituted DNA. Since Trp is frequently involved in protein–DNA interaction, Trp-induced EET assay can be a powerful tool for investigating protein–DNA interaction and possibly applied to many cases. To our knowledge, this

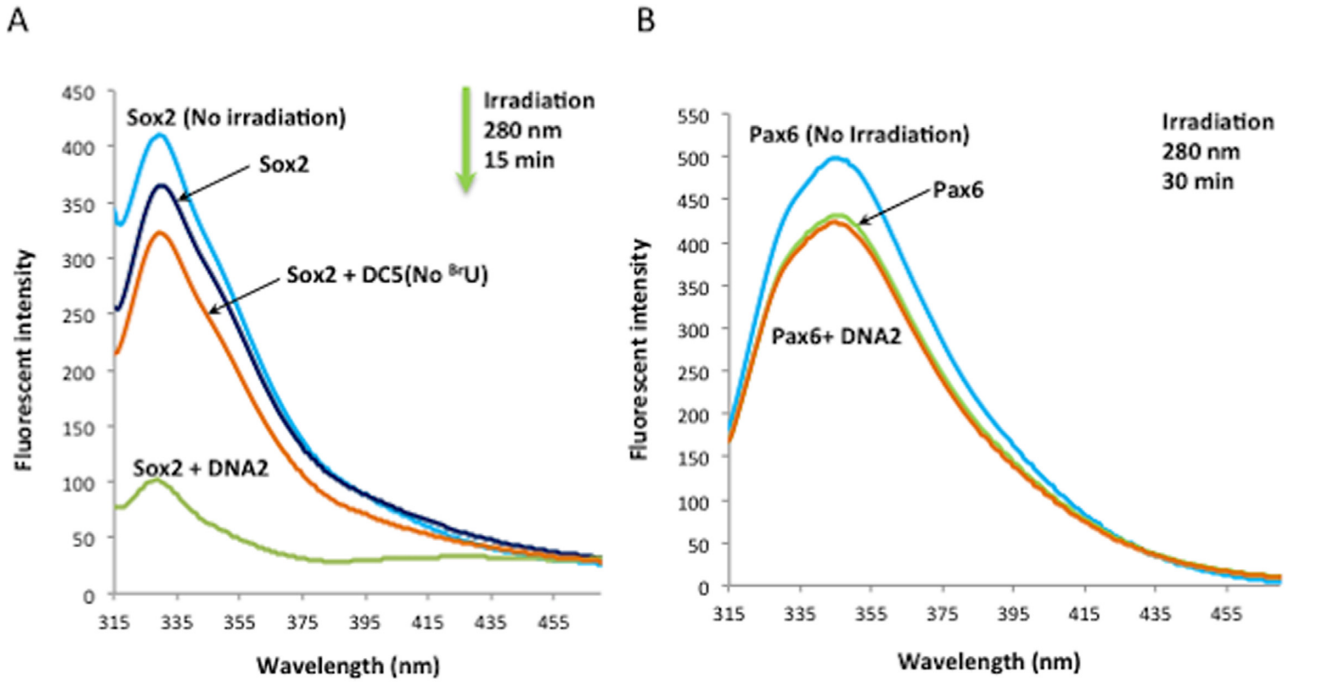

Figure 7. (**A**) Fluorescence intensity of tryptophan residues of Sox2. Fluorescence emission spectra of Sox2 before irradiation (blue) and after irradiation (dark blue) at 280 nm for 15 min. Emission spectra of Sox2 incubated with DNA2 (green) and with DC5 (orange), after irradiation for 15 min (excitation at 295 nm, 10 nm slit width). (**B**) Fluorescence emission spectra of Pax6 alone before irradiation (blue), after irradiation (green) and Pax6 when incubated with DNA2 irradiated at 280 nm for 30 min (orange) (excitation at 295 nm, 5 nm slit width). Photoreaction procedure for Sox2 and Pax6: reaction mixture was prepared using 20 mM sodium cacodylate buffer pH 7.50 and 2 μM of each protein and DNA in 50 μl (final volume), irradiated at 0°C.

is the first time to observe a crucial biological event such as cooperative binding of transcription factors to DNA using the EET assay. This study opens up ample opportunity to use EET as an efficient photosensitive method to probing DNA–protein interactions. Consequently, the application repertoire of this method can be expanded to various important biological events accompanied by a dynamic assembly of macromolecular complexes.

SUPPLEMENTARY DATA

Supplementary Data are available at NAR Online.

FUNDING

JSPS KAKENHI [24225005]; 'Basic Science and Platform Technology Program for Innovative Biological Medicine'; 'JSPS-NSF International Collaborations in Chemistry (ICC)' (to H.S.); Samsung Science & Technology Foundation [SSTF-BA1301-01 to K.K.K.]. Funding for open access charge: JSPS KAKENHI [24225005].
Conflict of interest statement. None declared.

REFERENCES

1. Levine,M. and Tjian,R. (2003) Transcription regulation and animal diversity. *Nature*, **424**, 147–151.
2. Vaquerizas,J.M., Kummerfeld,S.K., Teichmann,S.A. and Luscombe,N.M. (2009) A census of human transcription factors: function, expression and evolution. *Nat. Rev. Genet.*, **10**, 252–263.
3. Petti,A.A., McIsaac,R.S., Ho-Shing,O., Bussemaker,H.J. and Botstein,D. (2012) Combinatorial control of diverse metabolic and physiological functions by transcriptional regulators of the yeast sulfur assimilation pathway. *Mol. Biol. Cell*, **23**, 3008–3024.
4. Cunha,P.M.F., Sandmann,T., Gustafson,E.H., Ciglar,L., Eichenlaub,M.P. and Furlong,E.E.M. (2010) Combinatorial binding leads to diverse regulatory responses: Lmd is a tissue-specific modulator of Mef2 activity. *PLoS Genet.*, **6**, e1001014.
5. Reményi,A., Lins,K., Nissen,L.J., Reinbold,R., Schöler,H.R. and Wilmanns,M. (2003) Crystal structure of a POU/HMG/DNA ternary complex suggests differential assembly of Oct4 and Sox2 on two enhancers. *Genes Dev.*, **17**, 2048–2059.
6. Ng,C.K., Li,N.X., Chee,S., Prabhakar,S., Kolatkar,P.R. and Jauch,R. (2012) Deciphering the Sox-Oct partner code by quantitative cooperativity measurements. *Nucleic Acids Res.*, **40**, 4933–4941.
7. Kamachi,Y., Uchikawa,M., Tanouchi,A., Sekido,R. and Kondoh,H. (2001) Pax6 and SOX2 form a co-DNA-binding partner complex that regulates initiation of lens development. *Genes Dev.*, **15**, 1272–1286.
8. Narasimhan,K., Pillay,S., Huang,Y.H., Jayabal,S., Udayasuryan,B., Veerapandian,V., Kolatkar,P., Cojocaru,V., Pervushin,K. and Jauch,R. (2015) DNA-mediated cooperativity facilitates the co-selection of cryptic enhancer sequences by SOX2 and PAX6 transcription factors. *Nucleic Acids Res.*, **43**, 1513–1528.
9. Morimura,H., Tanaka,S., Ishitobi,H., Mikami,T., Kamachi,Y., Kondoh,H. and Inouye,Y. (2013) Nano-analysis of DNA conformation changes induced by transcription factor complex binding using plasmonic nanodimers. *ACS Nano*, **7**, 10733–10740.
10. Cvekl,A. and Ashery-Padan,R., (2014) The cellular and molecular mechanisms of vertebrate lens development. *Development*, **141**, 4432–4447.
11. Danno,H., Michiue,T., Hitachi,K., Yukita,A., Ishiura,S. and Asashima,M. (2008) Molecular links among the causative genes for ocular malformation: Otx2 and Sox2 coregulate Rax expression. *Proc. Natl. Acad. Sci. U.S.A.*, **105**, 5408–5013.
12. Shimozaki,K., Zhang,C.L., Suh,H., Denli,A.M., Evans,R.M. and Gage,F.H. (2012) SRY-box-containing gene 2 regulation of nuclear receptor tailless (Tlx) transcription in adult neural stem cells. *J. Biol. Chem.*, **287**, 5969–5978.

13. Lodato,M.A., Ng,C.W., Wamstad,J.A., Cheng,A.W., Thai,K.K., Fraenkel,E., Jaenisch,R. and Boyer,L.A. (2013) SOX2 co-occupies distal enhancer elements with distinct POU factors in ESCs and NPCs to specify cell state. *PLoS Genet.*, **9**, e1003288.
14. Yamamoto,S., De,D., Hidaka,K., Kim,K.K., Endo,M. and Sugiyama,H. (2014) Single molecule visualization and characterization of Sox2-Pax6 complex formation on a regulatory DNA element using a DNA origami frame. *Nano Lett.*, **14**, 2286–2292.
15. Sontz,P.A., Muren,N.B. and Barton,J.K. (2012) DNA charge transport for sensing and signalling. *Acc. Chem. Res.*, **45**, 1792–1800.
16. Andrew,W.A., Michael,A., Stephen,L.M., Robert,J.C. and Harry,B.G. (1988) Distance dependence of photoinduced long-range electron transfer in zinc/ruthenium-modified myoglobins. *J. Am. Chem. Soc.*, **110**, 435–439.
17. DeRosa,M.C., Sancar,A. and Barton,J.K. (2005) Electrically monitoring DNA repair by photolyase. *Proc. Natl. Acad. Sci. U.S.A.*, **102**, 10788–10792.
18. Boon,E.M., Livingston,A.L., Chimiel,N.H., David,S.S. and Barton,J.K., (2003) DNA-mediated charge transport for DNA repair. *Proc. Natl. Acad. Sci. U.S.A.*, **100**, 12543–12547.
19. Yavin,E., Boal,A.K., Stemp,E.D., Boon,E.M., Livingston,A.L., O'Shea,V.L., David,S.S. and Barton,J.K. (2005) Protein-DNA charge transport: redox activation of a DNA repair protein by guanine radical. *Proc. Natl. Acad. Sci. U.S.A.*, **102**, 3546–3551.
20. Kim,S., Li,Y. and Sancar,A., (1992) The third chromophore of DNA photolyase: Trp-277 of Escherichia coli DNA photolyase repairs thymine dimers by direct electron transfer. *Proc. Natl. Acad. Sci. U.S.A.*, **89**, 900–904.
21. Sancar,A. (2003) Structure and function of DNA photolyase and cryptochrome blue-light photoreceptors. *Chem. Rev.*, **103**, 2203–2237.
22. Behmoaras,T., Toulme,J.J. and Hélène,C. (1981) A tryptophan-containing peptide recognizes and cleaves DNA at apurinic sites. *Nature*, **292**, 858–859.
23. Wagenknecht,H.-A., Stemp,E.D.A. and Barton,J.K. (2000) Evidence of electron transfer from peptides to DNA: oxidation of DNA-bound tryptophan using the flash-quench technique. *J. Am. Chem. Soc.*, **122**, 1–7.
24. Wagenknecht,H.A., Rajski,S.R., Pascaly,M., Stemp,E.D. and Barton,J.K. (2001) Direct observation of radical intermediates in protein-dependent DNA charge transport. *J Am. Chem. Soc.*, **123**, 4400–4407.
25. Mayer-Enthart,E., Kaden,P. and Wagenknecht,H.A. (2005) Electron transfer chemistry between DNA and DNA-binding tripeptides. *Biochemistry.*, **44**, 11749–11757.
26. Tashiro,R., Wang,A.H. and Sugiyama,H. (2006) Photoreactivation of DNA by an archaeal nucleoprotein Sso7d. *Proc. Natl. Acad. Sci. U.S.A.*, **103**, 16655–16659.
27. Sugiyama,H., Tsutsumi,Y. and Saito,I. (1990) Highly sequence-selective photoreaction of 5-bromouracil-containing deoxyhexanucleotides. *J. Am. Chem. Soc.*, **112**, 6720–6721.
28. Sugiyama,H., Fujimoto,K. and Saito,I. (1996) Evidence for intrastrand C2′ hydrogen abstraction in photoirradiation of 5-halouracil-containing oligonucleotides by using stereospecifically C2′-deuterated deoxyadenosine. *Tetrahedron. Lett.*, **37**, 1805–1808.
29. Sugiyama,H., Tsutsumi,Y., Fujimoto,K. and Saito,I. (1993) Photoinduced deoxyribose C2′ oxidation in DNA. Alkali-dependent cleavage of erythrose-containing sites via a retroaldol reaction. *J. Am. Chem. Soc.*, **115**, 4443–4448.
30. Saha,A., Hashiya,F., Kizaki,S., Asamitsu,S., Hashiya,K., Bando,T. and Sugiyama,H. (2015) A novel detection technique of polyamide binding sites by photo-induced electron transfer in ^{Br}U substituted DNA. *Chem. Commun.*, **51**, 14485–14488.
31. Hashiya,F., Saha,A., Kizaki,S., Li,Y. and Sugiyama,H. (2014) Locating the uracil-5-yl radical formed upon photoirradiation of 5-bromouracil-substituted DNA. *Nucleic Acids Res.*, **42**, 13469–13473.
32. Xu,Y., Tashiro,R. and Sugiyama,H. (2007), Photochemical determination of different DNA structures. *Nat. Protoc.*, **2**, 78–87.
33. Watanabe,T., Bando,T., Xu,Y., Tashiro,R. and Sugiyama,H. (2005) Efficient generation of 2′-deoxyuridin-5-yl at 5′-(G/C)AA(X)U(X)U-3′ (X = Br, I) sequences in duplex DNA under UV irradiation. *J. Am. Chem. Soc.*, **127**, 44–45.
34. Watanabe,T., Tashiro,R. and Sugiyama,H. (2007) Photoreaction at 5′-(G/C)AA(Br)UT-3′ sequence in duplex DNA: efficient generation of uracil-5-yl radical by charge transfer. *J. Am. Chem. Soc.*, **129**, 8163–8168.
35. Lewis,F.D. and Wu,Y. (2001) Dynamics of superexchange photoinduced electron transfer in duplex DNAJ. *Photochem. Photobiol. C Photochem. Rev.*, **2**, 1–16.
36. Jolma,A., Yin,Y., Nitta,K.R., Dave,K., Popov,A., Taipale,M., Enge,M., Kivioja,T., Morgunova,E. and Taipale,J. (2015) DNA-dependent formation of transcription factor pairs alters their binding specificity. *Nature*, **527**, 384–388.